JOURNAL OF MATERIALS SCIENCE 26 (1991) 3400–3408

# Contribution to the study of reactive wetting in the CuTi/$Al_2O_3$ system

P. KRITSALIS, L. COUDURIER, N. EUSTATHOPOULOS
*Laboratoire de Thermodynamique et Physico-Chimie Métallurgiques, INP Grenoble, CNRS UA 29, ENSEEG, BP 75, 38402 Saint Martin d'Hères Cédex, France*

The wetting (kinetics of spreading and stationary contact angles) of CuTi alloys on monocrystalline alumina under high vacuum, at a temperature of 1373 K, by the sessile drop technique was investigated. The morphological and chemical characteristics of the metal–ceramic interface were determined by scanning electron microscopy and microprobe analysis. When the results are analysed, three distinct effects of the Ti solute on wetting can be identified and evaluated semi-quantitatively: (a) a reduction in the solid–liquid interfacial tension by adsorption into the liquid side of the interface; (b) a reduction in this tension by formation of a TiO metallic-like oxide layer in the solid side of the interface; (c) a contribution to the wetting driving force due to the free energy released at the interface by the reaction between Ti and $Al_2O_3$.

## 1. Introduction

The study of wettability of alumina by CuTi alloys is of great interest both in terms of its applications and its contribution to basic research. In fact, CuTi alloys are the basis of a great many alloys used for direct brazing of alumina and other ceramic materials [1, 2]. Moreover, the CuTi/$Al_2O_3$ system is typical of reactive wetting, that is of wetting accompanied by an irreversible change in the physicochemical nature of the interface. Despite the progress made regarding the theoretical description of this phenomenon [3–5], it is still not clear which of the following two factors is the decisive one:

(i) the standard Gibb's free energy value of the new phase formation reaction at the interface; the more negative this value, the smaller the contact angle of the metal of the ceramic. This idea gave rise to the so-called "quasi-chemical theory of wetting" [4, 6];

(ii) the electron structure of the interfacial reaction product. The more closely this structure resembles that of metals, the better the liquid metal wets the substrate [7].

There have been two major studies on the wetting properties of CuTi alloys on alumina. The first was conducted by Naidich and co-workers [4, 7] on monocrystalline alumina substrates under high vacuum. In addition to alumina, these authors also studied other refractory oxides ($SiO_2$, MgO and even certain titanium oxides, Table IV). The second study was undertaken by Nicholas and co-workers [8, 9] on polycrystalline alumina substrates, also under high vacuum. This study focused mainly on the effect of ternary solutes likely to reduce the Ti concentration needed to obtain a given level of wetting.

Despite certain quantitative differences between these two studies (for example, the Ti concentration required to obtain a 90° angle in the CuTi binary is 1 at % in [7] and 7 at % in [8]), there is agreement regarding the essential experimental results obtained by the addition of Ti:

(a) a large reduction in the Cu contact angle, from values much higher than 90° to just a few degrees; and

(b) the formation at the Cu/$Al_2O_3$ interface of an apparently continuous layer of a new phase, identified as the metallic-type oxide TiO [7].

In this paper an analysis of reactive wetting in the CuTi/$Al_2O_3$ system is given using results of previous studies as well as new results obtained in the present work. A special effort has been made to acquire data on wetting kinetics, which have not so far been available for this system.

## 2. Experimental procedure

The sessile drop method was used to study the influence of Ti on the contact angle, $\theta$, of the Cu/$Al_2O_3$ system at $T = 1373$ K between $X_{Ti} = 0$ and $X_{Ti} = 0.125$ ($X_{Ti}$ is the Ti molar fraction).

The experimental apparatus consists essentially of an alumina tube heated externally by a silicon carbide resistor. Windows are fitted at each end of this tube in order to illuminate and photograph the drop placed on the substrate or to project its image, magnified approximately 20 times, on to a screen to measure the contact angles. The tube is connected to a gas feed system and a vacuum device consisting of a vane pump and an oil diffusion pump, each pump being equipped with a liquid nitrogen trap. The experiments are conducted under a vacuum of $10^{-5}$–$10^{-4}$ Pa. The temperature is measured by a Pt/Pt–10% Rh thermocouple located in the immediate vicinity of the sample.

The substrates used are cylindrical platelets of $\alpha$-monocrystalline alumina (sapphire of 99.993% purity). The sapphire surface has a random crystallographic orientation, a fact which has no effect on $\theta$ in



0022–2461/91 $03.00 + .12 

view of the very low contact-angle anisotropy of liquid metals on alumina [10, 11]. After mechanical polishing, the average height of surface asperities on the platelets is 0.01 μm. Before the experiments, the substrates are ultrasound cleaned in acetone and then annealed under vacuum at 1473 K for 2 h in order to eliminate all work-hardening induced by the mechanical polishing and any hydroxyl groups that may have been adsorbed on the surface.

Drops of alloys of about 100 mg are prepared *in situ* by direct melting of Cu and Ti on the substrate. The copper contains less than 10 p.p.m. metallic impurities and 5–10 p.p.m. $O_2$. The Ti contains less than 400 p.p.m. metallic impurities and 600 ( $\pm$ 100) p.p.m. $O_2$.

The experiment consists in monitoring the time-dependent variation in contact angle while the temperature rises to $T = 1373$ K. The holding periods last for about 10–30 min, the time needed to obtain stationary angles being about 2 min.

## 3. Results

### 3.1. Contact angles

The photographs in Fig. 1 show how the fusion of a CuTi alloy takes place (a, b) and its spreading on the sapphire (c, d).

Fusion starts at the contact points between the Cu and Ti once the eutectic temperature ( $\approx$ 1145 K) of the phase diagram [12] is attained (Fig. 1a). As the temperature rises, the volume of liquid increases and the liquid/solid interface thus formed (Fig. 1b) moves towards the base of the sample until there is complete fusion at a temperature between that of the liquidus and that at which fusion of copper takes place. Once complete fusion is achieved, the contact angle instantaneously has a value, $\theta_0$, close to 90° (Fig. 1c, $t = 0$). The drop then spreads more slowly until a stationary angle, $\theta_{st}$, is reached (Fig. 1d, $t = 43$ s).

These wetting kinetics are practically the same for all $X_{Ti} \geqslant 0.05$ alloys. The initial angle, $\theta_0$, is equal to 90° $\pm$ 15°, a value much lower than that of the Cu/sapphire system at 1373 K ($\theta_{Cu} = 128° \pm 3°$). The angle $\theta_0$ is obtained in less than a second, which corresponds to an initial displacement rate of the triple line equal to or greater than about 1 mm $s^{-1}$.

The time ($t_{st}$) needed for the drop to reach the value $\theta_{st}$ is about $10^2$ s (Fig. 2, curve a), which represents an average triple line displacement rate two or three orders of magnitude lower than the initial rate.

When $\theta_{st}$ is reached, the contact angle hardly varies at all with time, even after 30 min at $T = 1373$ K.

For alloys with a low Ti concentration ($X_{Ti} < 0.05$), it has been noted that surface oxidation of the drop tends to take place. The angle thus formed upon fusion is very wide (about 140°) and when it starts to decrease the wetting kinetics are much slower (Fig. 2, curve b), undoubtedly influenced by the oxide layer still present on the liquid surface. Because the tendency towards oxidation is greater in alloys with the lowest Ti concentration (this point will be discussed further later), it was not possible to study alloys with $X_{Ti} < 0.025$.

Fig. 3 shows the stationary values of contact angles measured at 1373 K as a function of the Ti molar fraction. It can be seen that $\theta_{st}$ decreases quickly with the first additions of Ti and that hardly any further change takes place for $X_{Ti} > 0.10$. The 90° angle is obtained for $X_{Ti} \approx 0.015$, a value that is close to that

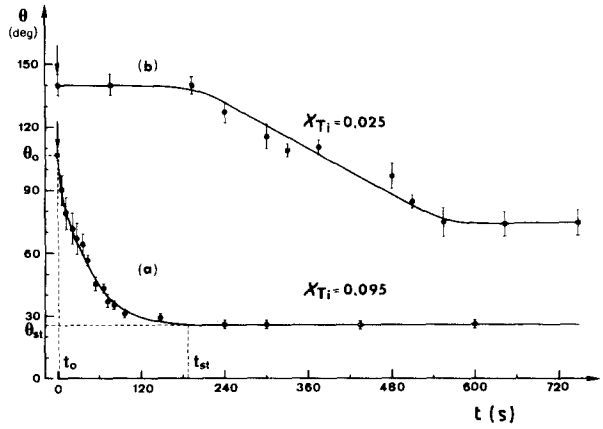


*Figure 2* (a) Typical variation of contact angle of a CuTi alloy on sapphire as a function of time. (b) Effect of a surface oxidation of the alloy on wetting kinetics. $T = 1373$ K.

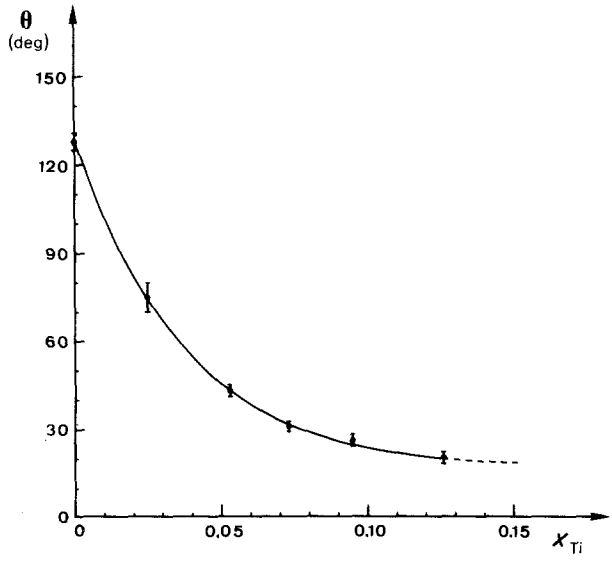


*Figure 3* Stationary contact angles of CuTi alloys on sapphire as a function of Ti molar fraction. $T = 1373$ K.

*Figure 1* Melting (a, b) and wetting (c, d) of a CuTi alloy ($X_{Ti} = 0.05$) on a sapphire substrate.

obtained by Naidich ($X_{Ti} = 0.010$) at a slightly higher temperature than in the present case (1423 K, as opposed to 1373 K) [4].

### 3.2. Characterization of the interface

Regardless of Ti concentration of the alloy, it still adheres strongly to the substrate. During cooling, stresses resulting from differences between the thermal expansion coefficients of the solidified alloy and the alumina cause the substrate to fracture a few hundred micrometres from the interface.

The micrographic observations made on a perpendicular section to the interface using a scanning electron microscope (SEM) show that for all alloys with $X_{Ti} \geqslant 0.050$ there are two distinct layers between the alumina and the alloy (Fig. 4): one layer that appears darker (layer I) at the contact with the alumina (black phase) and a lighter layer (layer II) between layer I and the alloy.

The $Al_2O_3$/layer I interface is not smooth. It has a roughness that is of the same size as the thickness of this layer, that is between 100 and 1000 nm, depending on the Ti concentration (Table I). This roughness is much greater than that of the initial surface of the alumina ( $\approx$ 10 nm).

Because layer I is very thin and varies a great deal from one point to another on the interface, it cannot be analysed quantitatively. In order to increase the thickness of this layer, a drop of $X_{Ti} = 0.125$ alloy was held on a sapphire substrate for 8 h at 1373 K. This was placed in an alumina crucible, with a cover to minimize evaporation of the liquid. After this holding period, the same type of interface was obtained with regard to the morphology of layers I and II, but the thickness of layer I had increased considerably while that of layer II did not change compared with a short experiment using an alloy with the same Ti concentration (Table I). This is clearly demonstrated by the concentration profiles obtained through the metal/ceramic interface using an electronic microprobe (Fig. 5). These profiles confirm the existence of two layers and enable identification of their composition: layer I is the titanium monoxide, $TiO_{1 \pm x}$, with $x \leqslant 0.05$. Layer II corresponds to the compound $Cu_2Ti_2O$ containing between 1 and 1.5 at % dissolved Al. The composition of this compound is closely related to, but different from, that of the compound $Cu_3Ti_3O$ mentioned in the literature [12] and obtained by quenching of CuTi alloys contaminated by oxygen.

*Figure 4* Scanning electron micrograph of CuTi(white)–$Al_2O_3$ (dark) showing two distinct layers at the interface ($X_{Ti} = 0.125$, $t \approx 10$ min).

TABLE I Thickness of layers I (TiO) and II ($Cu_2Ti_2O$) for different CuTi alloys. Holding time at 1373 K is $\approx$ 10 min, except for the last alloy marked by an asterisk (8 h)

| $X_{Ti}$ | $e^{I}$ (μm) | $e^{II}$ (μm) |
|---|---|---|
| 0.025 | – | $\approx 1$ |
| 0.050 | 0.1–0.3 | $\approx 2$ |
| 0.095 | 0.5–1.0 | $\approx 4$ |
| 0.126 | $\approx 1.0$ | $\approx 5$ |
| 0.125* | 4.0–5.0 | $\approx 5$ |

In alloy $X_{Ti} = 0.025$, only layer II appeared clearly at the interface. Layer I, if it exists, was not thick enough to be observed. However, by passing a probe through the metal/alumina interface in 0.5 μm steps, the existence of an area richer in Ti than layer II was found.

The influence of titanium concentration on the thickness of these layers is shown in Table I. Although it is difficult to measure accurately, the thickness of layer I seems to increase with $X_{Ti}$. The same is also true for layer II.

The lack of variation in the thickness of layer II with time would suggest that this layer does not form during the holding period at 1373 K but is produced by precipitation during cooling of the alloy. This layer thus has no influence on the wetting process but may influence the mechanical properties of the junction by virtue of the fact that it ensures a smoother transition between the ceramic and metallic phase.

## 4. Discussion

### 4.1. Thermodynamics

The chemical interaction in the system studied can be described by the dissolution of the alumina in the alloy

$$Al_2O_3 \rightarrow 2(Al) + 3(O) \quad (1)$$

followed by precipitation of a Ti oxide (TiO or $Ti_2O_3$ or even $Ti_3O_5$) at the interface, for example

$$(Ti) + (O) \rightarrow TiO \quad (2)$$

In equations 1 and 2, the parentheses indicate that the Al, Ti and O species are in dissolved form in the liquid alloy.

Using the thermodynamic data in Table II, the variation in oxygen activity, $a_O$, (reference state: oxygen at infinite dilution) in equilibrium with the alumina was calculated (Appendix 1) as a function of $X_{Al}$ in the liquid alloy. This function is represented logarithmically by the straight line A (Fig. 6). Likewise, the variation in oxygen activity in equilibrium with the different Ti oxides as a function of $X_{Ti}$ is represented by the sequence of the segments $B_1B_2$(TiO), $B_2B_3$($Ti_2O_3$) and $B_3B_4$($Ti_3O_5$).

The same figure also shows curve B′, giving the oxygen molar fraction, $X_O$, in equilibrium with TiO or

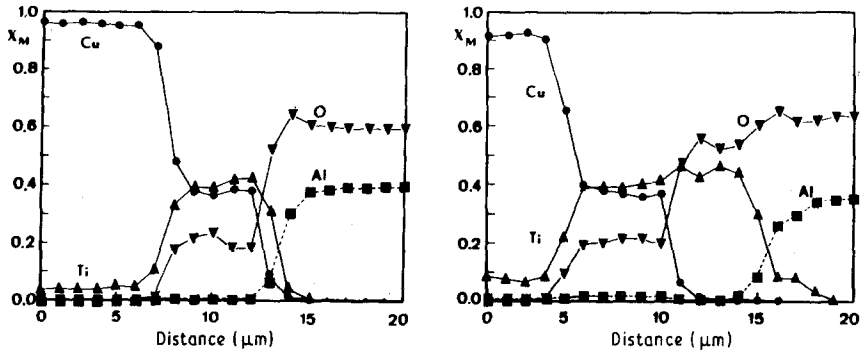


*Figure 5* $Al_2O_3$–CuTi ($X_{Ti} \approx 0.125$) interface with corresponding microprobe line scans of composition in molar fraction. Holding time at 1373 K, (a) 10 min and (b) 8 h. (●) Cu, (▲) Ti, (▼) O, (■) Al.

TABLE II Thermochemical data at $T = 1373$ K used to calculate the curves in Fig. 6. Parentheses denote liquid and ⟨ ⟩ solid

| Reaction | Gibb's free energy (kJ) | Reference |
|---|---|---|
| $(Ti) = (Ti)_{Cu}$ | $\overline{\Delta G}^{E_x}_{(Ti)Cu} = -24.287$ | [13] |
| $\frac{1}{2}O_2 = (O)_{Cu}$ | $\overline{\Delta G}^{E_x}_{(O)Cu} = -22.504$ | [14] |
| $(Al) = (Al)_{Cu}$ | $\overline{\Delta G}^{E_x}_{(Al)Cu} = -69.622$ | [15] |
| $(Ti) + \frac{1}{2}O_2 = \langle TiO \rangle$ | $\Delta G^\circ_f = -412.216$ | [16] |
| $\frac{2}{3}(Ti) + \frac{1}{2}O_2 = \frac{1}{3}\langle Ti_2O_3 \rangle$ | $\Delta G^\circ_f = -384.874$ | [16] |
| $\frac{3}{5}(Ti) + \frac{1}{2}O_2 = \frac{1}{5}\langle Ti_3O_5 \rangle$ | $\Delta G^\circ_f = -373.712$ | [16] |
| $\frac{2}{3}(Al) + \frac{1}{2}O_2 = \frac{1}{3}\langle Al_2O_3 \rangle$ | $\Delta G^\circ_f = -410.264$ | [16] |

$Ti_2O_3$. The equations for curve B′ are deduced from those representing the straight lines B by a calculation described in Appendix 1.

In view of the approximations made in the calculation, the uncertainty in the exact position of this curve is high (estimated at about a factor of 10). Despite this lack of certainty, curve B′ clearly indicates that the oxygen solubility in the CuTi alloy in equilibrium with $Ti_2O_3$ or TiO increases rapidly as soon as $X_{Ti}$ is above $10^{-4}$. This increase is the result of very strong interactions between the O and Ti atoms dissolved in Cu, as indicated by the very negative value of the interaction parameter $\varepsilon_O^{Ti} \approx -10^4$ [17].

The curves in Fig. 6 will now be used to explain certain observations made during experiments.

First, it must be remembered that in the experiments described here, the CuTi alloys tended to oxidize during their formation. This tendency was more marked in alloys with the lowest Ti concentration. CuTi alloys do, in fact, contain a certain oxygen concentration, $X_O^*$, at the outset, introduced mainly through the titanium (oxygen is a common impurity of Ti) and represented in Fig. 6 by curve C. If, at a given value of $X_{Ti}$, $X_O^*$, is higher than the value of $X_O$ given for curve B′, the dissolved oxygen may react with the titanium and form an oxide film on the surface of the liquid which could block the spreading of the drop. The shape of curves B′ and C clearly indicates that surface oxidation of CuTi alloys is more likely to occur when the Ti concentration is low, which coincides with the experimental observations. More generally, this analysis shows that for brazing operations it is advantageous to work with titanium-rich CuTi alloys, not only to improve wetting (in reality, for $X_{Ti} > 0.10$, $\theta_{st}$ virtually no longer varies as a function of $X_{Ti}$) but also to avoid surface oxidation of the liquid alloy.

It is also worth noting that the straight lines B in Fig. 6 are situated below the straight line A describing the alumina dissolution equilibrium (Equation 1). For a given $O_2$ activity, Fig. 6 shows that, at equilibrium, the molar fraction of Al is higher than that of Ti. (For example, for $X_{Ti} = 10^{-2}$, $X_{Al} = 4 \times 10^{-2}$). As the alumina dissolves in the liquid, the $O_2$ in solution reacts with Ti and forms a titanium oxide, while the remaining alloy becomes richer in Al. In fact, the analyses revealed that even after a holding period of 8 h at 1373 K, the Al concentration in the alloy was still low compared with the expected value at equilibrium. This was probably due to the fact that, after a transition period, the reaction continued very slowly by diffusion through the continuous layer of titanium oxide formed at the interface.

According to thermodynamic calculations, this oxide should be the monoxide TiO for $X_{Ti} > 2 \times 10^{-3}$, which corresponds to the $X$-value of point $B_2$, Fig. 6.

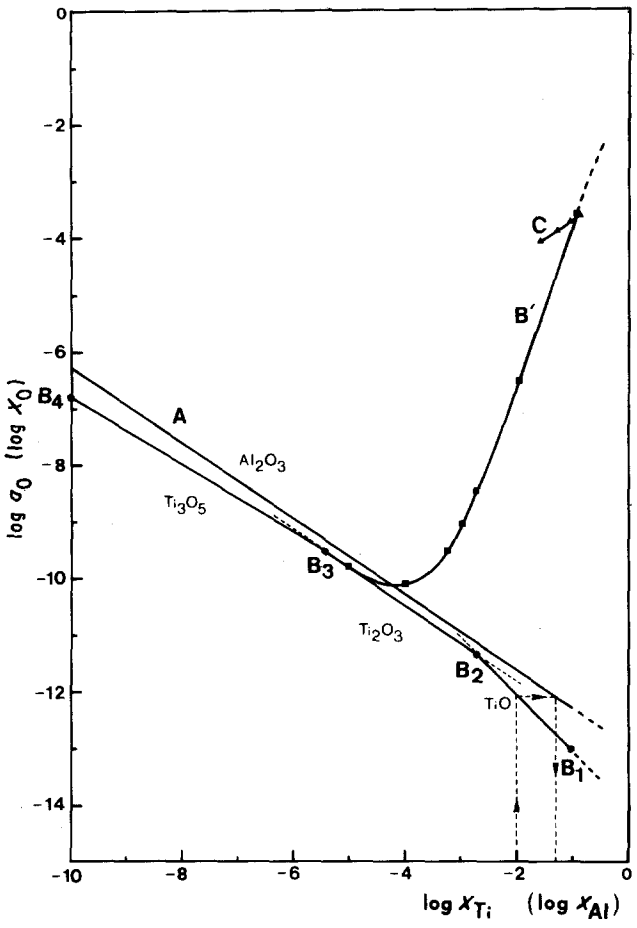


*Figure 6* Thermodynamics of $CuTi/Al_2O_3$ system at 1373 K. Straight line A represents logarithmically thermodynamical activity, $a_O$, of oxygen in CuTi alloys in equilibrium with $Al_2O_3$ as a function of $X_{Al}$. Segments $B_3B_4$, $B_2B_3$ and $B_1B_2$ describe the variation of $a_O$ in equilibrium with the different Ti oxides as a function of $X_{Ti}$. For the same equilibria, curve B' gives the variation of molar fraction of oxygen $X_O$ as a function of $X_{Ti}$. Curve C represents the molar fraction of oxygen introduced in the CuTi alloys through the titanium.

Below this value and to about $4 \times 10^{-6}$ (point $B_3$), the stable oxide is $Ti_2O_3$. Note that the analyses showed without any doubt that the oxide formed at the interface is indeed TiO for $X_{Ti} \approx 0.12$, but there are experimental occurrences (particularly the morphological similarity) that suggest that the same would be true for $X_{Ti} \geqslant 0.05$.

## 4.2. Analysis of reactive wetting

In the absence of a chemical reaction, the equilibrium contact angle, $\theta'$, is related to the solid–vapour, $\sigma_{SV}$, liquid–vapour $\sigma_{LV}$, and solid–liquid, $\sigma_{SL}$, surface tensions by the classical equations

$$\cos\theta' = \frac{\sigma_{SV} - \sigma_{SL}}{\sigma_{LV}} = \frac{W}{\sigma_{LV}} - 1 \quad (3)$$

where $W$ is the work of adhesion defined by

$$W = \sigma_{SV} + \sigma_{LV} - \sigma_{SL} \quad (4)$$

When wetting is accompanied by the formation of a new phase at the interface, the contact angle may reach a value $\theta$, given by the expression [5]

$$\cos\theta = \cos\theta' - \frac{\Delta\sigma_r}{\sigma_{LV}} - \frac{\Delta F_r}{\sigma_{LV}} \quad (5)$$

in which the last two terms represent the effect of the chemical reaction on wetting. The term $\Delta F_r$ is the result of the free energy released by the reaction

$$3(Ti) + Al_2O_3 \rightarrow 3TiO + 2(Al) \quad (6)$$

In fact, under certain conditions, which were discussed previously [3, 5], this energy may be transformed at the interface into surface energy that can be used for spreading. The term $\Delta\sigma_r$ takes into account the variation in $\sigma_{SL}$ due to the change in the physicochemical nature of the interface

$$\Delta\sigma_r = (\sigma_{Al_2O_3/TiO} + \sigma_{CuTi/TiO}) - \sigma_{CuTi/Al_2O_3} \quad (7)$$

Before discussing the terms $\Delta\sigma_r$ and $\Delta F_r$ it is important to specify the meaning of the angle $\theta'$ in the case that has been studied. This is the contact angle formed by a CuTi alloy on alumina in the absence of a chemical reaction at the interface. Taking into account the $\theta(t)$ kinetic results obtained, $\theta'$ is identified with the angle $\theta_0$ observed instantaneously after complete fusion of the drop. Thus, for $X_{Ti} \geqslant 0.05$ alloys, $\theta = 90° \pm 15°$, a value much lower than that measured for pure copper ($128° \pm 3°$). By taking a $\sigma_{LV}$ value equal to 1300 mJ m$^{-2}$ for Cu and CuTi alloys (small additions of Ti in Cu cause virtually no change in the surface tension of this metal [7]), it is found that, by using Equation 3, the addition of Ti in Cu results in a reduction in $\sigma_{SL}$ (or an equivalent increase in $W$) of about 800 mJ m$^{-2}$.

This decrease in $\sigma_{SL}$ is thus due to a simple Ti adsorption process at the $Cu/Al_2O_3$ interface. In fact, the results of the experiments given in Table III for three AB/sapphire systems (where B is a metallic solute that does not react with the substrate but which has a much higher work of adhesion value than that of the A matrix) show that such a process can cause very wide variations in contact angle and $\sigma_{SL}$. The value of $W_{Ti}$ on $Al_2O_3$ in the absence of a reaction is obviously not known, because the $Ti/Al_2O_3$ pair reacts at any temperature. However, it is possible to estimate this value by using the expression established by Chatain *et al.* [21] for estimating the work of adhesion of non-reactive metals on alumina. The calculated value, equal to 1400 mJ m$^{-2}$ (Appendix 2), is much greater than that of copper ($W_{Cu} \approx 500$ mJ m$^{-2}$), so that the hypothesis regarding Ti adsorption at the $Cu/Al_2O_3$ interface can be justified, at least qualitatively.

If the value of $\theta'$ (90°) is included in Equation 5, the effect of Reaction 6 on wetting of alumina by a CuTi alloy at 10 at % of Ti (for which $\theta_{st} = 23°$) is equal to

$$\Delta\sigma_r + \Delta F_r = -\Delta W_r = -1200 \text{ mJ m}^{-2} \quad (8)$$

To assess the respective contributions of $\Delta\sigma_r$ and $\Delta F_r$, our experimental results regarding wetting on $Al_2O_3$ will be used in conjunction with the results obtained by Naidich for TiO wettability by Cu and CuTi alloys (Appendix 3). In view of the approximations that have

TABLE III Influence of the addition of 10 at % solute B in matrix A on the interfacial tension, $\sigma_{SL}$, and the contact angle of the A/$Al_2O_3$ system

| System A–B | $T$ (K) | $\theta_A$ (deg) | $W_A$ (mJ m$^{-2}$) | $W_B$ (mJ m$^{-2}$) | $X_B = 0.10$ | | Ref. |
|---|---|---|---|---|---|---|---|
| | | | | | $\Delta\sigma_{SL}$ (mJ m$^{-2}$) | $\Delta\theta$ (deg) | |
| Sn–Al | 1373 | 122 | 225 | 950 | − 400 | − 45 | [18] |
| Au–Si | 1373 | 139 | 280 | 900 | − 600 | − 35 | [19] |
| Cu–Al | 1523 | 129 | 475 | 1000 | − 575 | − 25 | [20] |

been made, there is considerable uncertainty surrounding each of the terms $\Delta\sigma_r$ and $\Delta F_r$ and only their upper and lower limits can be calculated

$$-1000 < \Delta\sigma_r < -600 \quad (9a)$$

$$-600 < \Delta F_r < -200 \quad (9b)$$

Thus, in the case in question, the two contributions of the interfacial reaction to wetting tend to decrease the contact angle. The extremely negative value of $\Delta\sigma_r$ after replacement of $Al_2O_3$ by TiO (Equation 7) is undoubtedly linked to the metallic character of TiO that has been mentioned elsewhere [7]. Indeed, it appears reasonable to assume that the interactions between a metal and this type of oxide are much stronger than those between the same metal and an ionocovalent oxide such as $Al_2O_3$ or $Ti_2O_3$ (Table IV).

Moreover, the term $\Delta F_r$, although not negligible, is relatively small compared with the other Ti effects. For an alloy containing 10 at % Ti, $\Delta F_r$ represents less than 30% of the total increase in $W$ due to the addition of Ti. This weak influence of $\Delta F_r$ is not surprising, because the standard Gibb's free energy of Reaction 6 is itself very small ($-2$ kJ mol$^{-1}$ TiO formed).

The results of this analysis are presented in diagrammatic form in Fig. 7. In this figure, ABC is a wetting path obtained from our results for two independent experiments: the first (A), concerns pure copper on $Al_2O_3$, the second (B, C), concerns the CuTi alloy on $Al_2O_3$. Note that here B and C are two successive steps of a single experiment.

The path AB′C′ represents the results of three independent experiments conducted by Naidich [4]: pure copper on $Al_2O_3$(A), pure copper on TiO(B′) and CuTi on TiO(C′). For this path, the term $\Delta F_r$ is negligible because of the absence of a chemical reaction at the interface (only slight dissolution of TiO in the alloy can take place). The passage from 128° to 30° is, in this case, due to the $\sigma_{SV}$ and $\sigma_{SL}$ variations following the replacement of alumina by TiO (stage b′), on the one hand, and the adsorption of Ti at the Cu/TiO interface on the other (stage a′). It can be seen that paths ABC and AB′C′ are equivalent in terms of energy, both in terms of total variation of $W$ as well as partial variations of this quantity. This comparison confirms the main findings of the analysis, namely that the role of Ti on wetting in the Cu/$Al_2O_3$ system consists essentially in modifying the interface. This modification takes place as a result of the two effects shown in the diagram in Fig. 8. The first involves the modification of the liquid side of the interface by

TABLE IV Contact angles and work of adhesion of Cu on alumina and titanium oxides at 1423 K [4]

| Oxide | $\theta$ (deg) | $W$ (mJ m$^{-2}$) |
|---|---|---|
| $Al_2O_3$ | 129 | 461 |
| $Ti_2O_3$ | 113 | 739 |
| $TiO_{1.14}$ | 82 | 1458 |
| $TiO_{0.86}$ | 72 | 1651 |

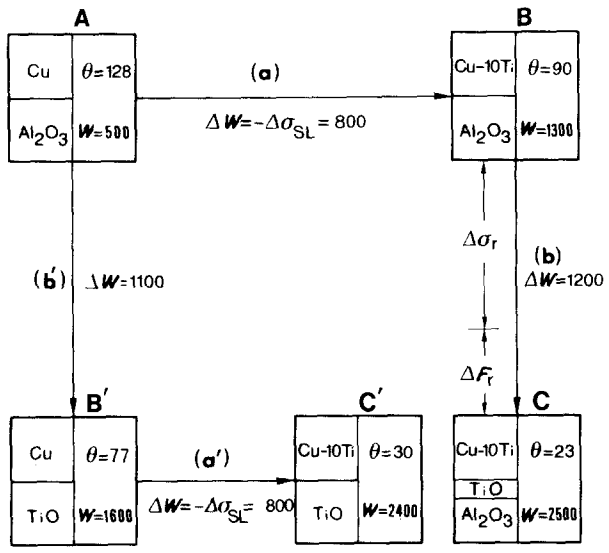


*Figure 7* Comparison between two wetting paths, ABC (this work) and AB′C′ [4].

creating through segregation, a layer of liquid with a high Ti concentration. The thickness of this layer is equivalent to that of an adsorption layer, typically about a nanometre. Considering the strong interactions between Ti and O, the Ti enrichment of this layer must also lead to its oxygen enrichment. The second influence of Ti involves the modification of the solid side of the interface by local replacement of alumina with TiO. It can be seen that the resulting chemical interface is far more diffuse than the initial interface. This interface provides a smoother transition in the chemical bond from an ionocovalent bond, in the alumina, to a metallic bond, in the alloy.

## 5. Conclusions

The wetting kinetics of CuTi alloys on alumina, studied at $T = 1373$ K, can be divided into two stages:

(i) a first stage (typical time = 1 s) involving the adsorption of Ti at the Cu/$Al_2O_3$ interface;

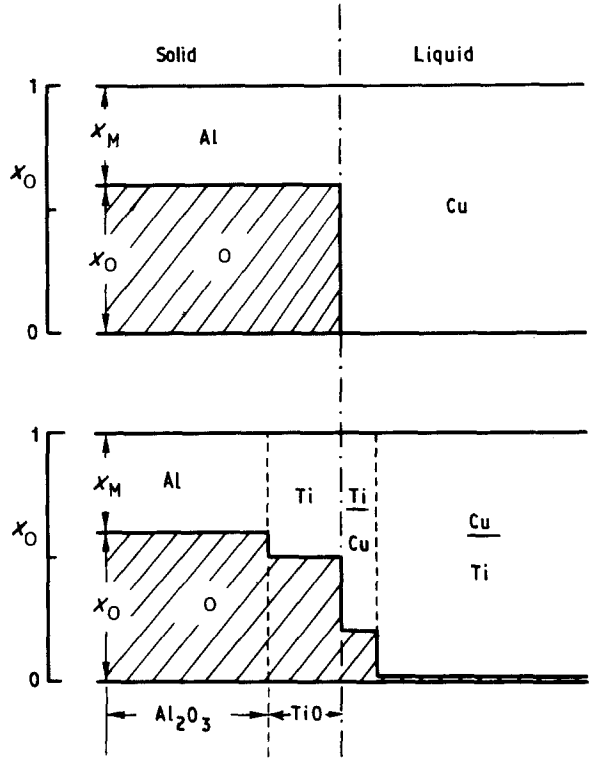


*Figure 8* Schematic description of oxygen molar fraction profile across a solid alumina–liquid copper interface (top) and a solid alumina–liquid CuTi interface (bottom). *M* is the metal complement to oxygen at any point.

(ii) a second, slower stage (typical time = $10^2$ s) involving the reaction with the substrate.

After cooling, the interface consists of two macroscopic layers. The first, formed at the contact with the substrate, is identified as TiO and results from the alumina reduction reaction by titanium. The thickness of this layer depends on the Ti concentration in the alloy and the holding time at the temperature of the experiment. The second layer corresponds to the $Cu_2Ti_2O$ compound. Its thickness increases with Ti concentration but it is not dependent upon holding time. This layer precipitates from the alloy during cooling.

The addition of 10 at % Ti in Cu leads to a decrease in the contact angle from $\approx 130°$ to $\approx 25°$ and an increase in the work of adhesion by a factor of 5. It has been shown that only a small part of this increase in $W$ can be attributed to the free energy of the reaction between Ti and $Al_2O_3$ released at the interface. Most of the increase can be attributed to the reduction in $Cu/Al_2O_3$ interfacial tension due to the *in situ* modification of both the liquid and solid sides of the interface by the titanium: the formation of an adsorption layer rich in Ti and $O_2$ in the liquid side and a metallic-like oxide, TiO, in the solid side of the interface.

## Acknowledgements

The authors thank Mrs N. Valignat and Mr J. Garden for their much appreciated assistance with the characterization of the interfaces, and the Bodosaki's foundation, for the research grant awarded to P. Kritsalis.

## Appendix 1

The thermodynamic equilibrium condition for Reaction 1 involving the dissolution of alumina in the Cu–Ti alloy is written as follows

$$\ln(a'^3_O\ a'^2_{Al}) = \frac{\Delta G^\circ_f}{RT} \quad (A1)$$

where $\Delta G^\circ_f$ is the standard Gibb's free energy of formation of alumina (Table II), $a'_{Al}$ is the thermodynamic activity of Al in the alloy (reference state: pure Al), and $a'_O$ that of dissolved $O_2$ (reference state: pure gaseous oxygen at a pressure of 1 atm).

To simplify the graphic representation of Equation A1, these activities can be replaced by activities defined by the following change in reference state

$$a_O = \frac{a'_O}{\gamma'_{(O)Cu}} = \frac{\gamma'_O}{\gamma'_{(O)Cu}} X_O \quad (A2a)$$

$$a_{Al} = \frac{a'_{Al}}{\gamma'_{(Al)Cu}} = \frac{\gamma'_{Al}}{\gamma'_{(Al)Cu}} X_{Al} \quad (A2b)$$

where $\gamma'_{(O)Cu}$ and $\gamma'_{(Al)Cu}$ are constants representing the activity coefficients of the oxygen and aluminium at infinite dilution in pure copper. These values are estimated using corresponding values of partial excess free enthalpy of mixing at infinite dilution (Table II).

$$RT \ln \gamma'_{(O)Cu} = \overline{\Delta G}^{E_x}_{(O)Cu} \quad (A3a)$$

$$RT \ln \gamma'_{(Al)Cu} = \overline{\Delta G}^{E_x}_{(Al)Cu} \quad (A3b)$$

Taking into account Relationships A2 and A3, Equation A1 is written

$$\ln a_O = \frac{\Delta G^*}{3RT} - \frac{2}{3} \ln a_{Al} \quad (A4)$$

where $\Delta G^* = \Delta G^\circ_f - 3\overline{\Delta G}^{E_x}_{(O)Cu} - 2\overline{\Delta G}^{E_x}_{(Al)Cu}$

The coefficient $\gamma'_{Al}$ in Equation A2b varies, in theory, with the composition of the Cu–Ti alloy. However, because the molar fraction of Ti is low ( $< 0.12$), $\gamma'_{Al}$ is akin to $\gamma'_{(Al)Cu}$, so that $a_{Al} \approx X_{Al}$. Equation A4 is then written as

$$\ln a_O = 29.9 - \tfrac{2}{3} \ln X_{Al} \quad (A5)$$

This equation is represented by the straight line A in Fig. 6.

The equilibrium equation for Reaction 2 is calculated in the same way as previously

$$\ln a_O = 32.4 - \ln X_{Ti} \quad (A6)$$

This relationship is represented by the straight line $B_1B_2$ in Fig. 6.

The calculation is repeated assuming that the Ti oxide formed by precipitation is $Ti_2O_3$ (straight line $B_2B_3$) or $Ti_3O_5$ (straight line $B_3B_4$).

In order to calculate the oxygen molar fraction in equilibrium with TiO by means of Equation A6, the $\gamma'_O/\gamma'_{(O)Cu}$ ratio has to be estimated. A formalism involving the interaction parameters is generally used for this calculation

$$\ln \frac{\gamma'_{(O)}}{\gamma'_{(O)Cu}} = \varepsilon^{Ti}_O X_{Ti} + \frac{1}{2} \rho^{Ti}_O X^2_{Ti} + \cdots \quad (A7)$$

where $\varepsilon_O^{Ti}$ and $\rho_O^{Ti}$ are the first- and second-order O–Ti interaction parameters, respectively. The experimental value of $\varepsilon_O^{Ti}$ is very negative ( − 9600 [17]), but that of $\rho_O^{Ti}$ is not known, which means that it is impossible to apply Equation A7 for $X_{Ti} > 10^{-3}$. For this reason, an equation established using the model given by Jacob and Alcock [22] has been used

$$\ln \frac{\gamma'_{(O)}}{\gamma'_{O_{(Cu)}}} = -4 \ln\left(1 - \frac{\varepsilon_O^{Ti}}{4} X_{Ti}\right) \quad \text{(A8)}$$

taking for $\varepsilon_O^{Ti}$ the experimental value of − 9600.

By means of Equations A8 and A6, $\ln X_O$ is calculated as a function of $\ln X_{Ti}$. The resulting curve B' is extremely approximate because, on the one hand, the uncertainty in the experiment regarding the interaction parameters ε is generally very high and, on the other hand, Equation A8 is not a precise equation but is based on a model.

## Appendix 2

In the thermodynamic model given by Chatain *et al.* [21], the work of adhesion of a metal, Me, on alumina is given by the expression.

$$W = \frac{1}{\Omega_{Me}} \left\{ 0.08 \Delta H^{\circ}_{f_{(MeO)}} + 0.15 \overline{\Delta H}^{\infty}_{Al_{(Me)}} \right\} \quad \text{(A9)}$$

where $\Omega_{Me}$ is the molar surface area of the metal (calculated from the molar volume of the metal, $V_{Me}$, by the expression $\Omega_{Me} = 1.091\, N (V_{Me}/N)^{2/3}$, where $N$ is Avogadro's number), $\Delta H^{\circ}_{f(MeO)}$ is the enthalpy of formation of the MeO oxide, and $\overline{\Delta H}^{\infty}_{Al(Me)}$ the partial mixing enthalpy of Al at infinite dilution in the liquid metal.

If the following values are taken: $\Omega_{Ti} = 4.5 \times 10^4\ m^2\ mol^{-1}$, $\Delta H^{\circ}_{f(TiO)} = -549\ kJ$ at O [16], $\overline{\Delta H}^{\infty}_{Al(Ti)} = -147\ kJ\ mol^{-1}$ [23], then $W_{Ti} \approx 1400\ mJ\ m^{-2}$.

Note that in order to make a complete calculation of Ti adsorption at the $Cu/Al_2O_3$ interface, not only must the values $W_{Cu}$ and $W_{Ti}$ be considered, but also the bond energies of these metals as well as the Cu–Ti interaction energy [24]. However, the condition $W_{Ti} \gg W_{Cu}$ is sufficient in the present case for qualitative determination of Ti adsorption at the $Cu/Al_2O_3$ interface.

## Appendix 3

Equation 7 brings into play the $Al_2O_3/TiO$ interface tension. To our knowledge, there are no data on interface tensions where the two phases in contact are oxides. Taking into account current knowledge of metallic interphases [25, 26], an upper limit for $\sigma_{Al_2O_3/TiO}$ would be given by the value of the grain-boundary tension of a refractory oxide, namely a few hundreds of $mJ\ m^{-2}$. Such a value would correspond to the case where no preferential orientation relation exists between the phases in contact. The nucleation and growth of the first layers of a crystalline phase (in this case TiO) on a substrate (here $Al_2O_3$) generally take place through the formation of coherent interfaces with tensions that may be one order of magnitude lower than those of incoherent interphases [25, 26].

For this reason, this tension has not been taken into account in the semiquantitative analysis. Equation 7 can therefore be written

$$\Delta\sigma_r \approx -(\sigma_{CuTi/Al_2O_3} - \sigma_{CuTi/TiO}) \quad \text{(A10)}$$

In order to estimate this difference, the results obtained by Naidich (Table IV) have been used concerning pure copper on $Al_2O_3$ and on different Ti oxides. It was found that when $Al_2O_3$ is replaced by an oxide closely related to TiO, the work of adhesion increases by $\approx 1100\ mJ\ m^{-2}$. This increase is written as follows

$$1100 \approx (\sigma_{TiO/V} - \sigma_{Al_2O_3/V}) + (\sigma_{Cu/Al_2O_3} - \sigma_{Cu/TiO}) \quad \text{(A11)}$$

Alumina surface tension values $\sigma_{Al_2O_3/V}$ in the experiments presented in the literature vary from 700–1000 $mJ\ m^{-2}$ [27–30], while that of TiO is not known. Because the surface tensions of refractory oxides are usually between 700 and 1200 $mJ\ m^{-2}$ [31], the maximum difference between the surface tensions of the oxides TiO and $Al_2O_3$ have been estimated to be 500 $mJ\ m^{-2}$. A lower limit for the difference in interface tensions can thus be obtained

$$\sigma_{Cu/Al_2O_3} - \sigma_{Cu/TiO} \geqslant 600\ mJ\ m^{-2} \quad \text{(A12)}$$

The introduction of Ti in the copper definitely modifies each of the interfacial tensions in Equation A12, but it has little influence on the difference between the two measurements. This is quite clear if the values of $\Delta\sigma_{SL} = -\Delta W$ are compared in steps a and a' on the diagram in Fig. 7 and, consequently

$$-\Delta\sigma_r = (\sigma_{CuTi/Al_2O_3} - \sigma_{CuTi/TiO}) \geqslant 600\ mJ\ m^{-2} \quad \text{(A13)}$$

This inequality, introduced in Equation 8, provides a means of estimating the upper limit of $|\Delta F_r|$ ($\Delta F_r$ is, by definition, a negative quantity)

$$|\Delta F_r| \leqslant 600\ mJ\ m^{-2} \quad \text{(A14)}$$

To estimate the lower limit of $|\Delta F_r|$, Equation 3 is replaced in Equation 5. Thus

$$\sigma_{Al_2O_3/V} - \{(\sigma_{Al_2O_3/TiO} + \sigma_{CuTi/TiO}) + \Delta F_r\} - \sigma_{LV} \cos\theta = 0 \quad \text{(A15)}$$

or

$$\sigma_{Al_2O_3/TiO} + \sigma_{CuTi/TiO} = \sigma_{Al_2O_3/V} - \sigma_{LV} \cos\theta - \Delta F_r \quad \text{(A16)}$$

The left-hand side of this equation is, by definition, a positive quantity, which results in the following inequality

$$|\Delta F_r| > \sigma_{LV} \cos\theta - \sigma_{Al_2O_3/V} \quad \text{(A17)}$$

Because the maximum surface tension value of alumina is equal to 1000 $mJ\ m^{-2}$, it is found that

$$|\Delta F_r| > 200\ mJ\ m^{-2} \quad \text{(A18)}$$

and, taking into account Equation A14

$$200 \leqslant |\Delta F_r| \leqslant 600 \quad \text{(A19)}$$

Because it was seen that the total variation in $W$ during the reactive stage (stage b in Fig. 7) is 1200 mJ $m^{-2}$, the following range for $|\Delta\sigma_r|$ is obtained

$$600 \leqslant |\Delta\sigma_r| \leqslant 1000 \qquad \text{(A20)}$$

## References


1. M. G. NICHOLAS, *Br. Ceram. Trans. J.* **85** (1986) 144.
2. A. J. MOORHEAD, *Adv. Ceram. Mater.* **2** (1987) 159.
3. I. J. ASKAY, C. E. HOGE and J. A. PASK, *J. Phys. Chem.* **78** (1974) 1178.
4. YU. V. NAIDICH, *Prog. Surf. Membr. Sci.* **14** (1981) 353.
5. V. LAURENT, Thesis, INP Grenoble, France (1988).
6. YU. V. NAIDICH and YU. N. CHUVASHOV, *J. Mater. Sci.* **18** (1983) 2071.
7. YU. V. NAIDICH, V. S. ZHURAVLEV, V. G. CHUPRINA and L. V. STRASHINSKAYA, *Poroshkovaya Metallurgiya* **131** (11) (1973) 40.
8. R. STANDING and M. NICHOLAS, *J. Mater. Sci.* **13** (1978) 1509.
9. M. G. NICHOLAS, T. M. VALENTINE and M. J. WAITE, *J. Mater. Sci.* **15** (1980) 2197.
10. D. CHATAIN, I. RIVOLLET and N. EUSTATHOPOULOS, *J. Chim. Phys.* **84** (1987) 201.
11. P. OWNBY and J. LIU, *J. Adhesion Sci. Technol.* **2** (1988) 255.
12. M. HANSEN, "Constitution of Binary Alloys", Materials Science and Engineering Series (McGraw-Hill, New York, 1958).
13. J. L. MURRAY, *Bull. Alloy Phase Diagr.* **4**(1) (1983) 81.
14. R. SCHMID, *Metall. Trans.* **14B** (1983) 473.
15. R. HULTGREN, P. D. DESAI, D. T. HAWKINS, M. GLEISER and K. K. KELLY, "Selected values of the Thermodynamic Properties of Binary Alloys" (American Society for Metals, Metals Park, Ohio, 1973).
16. JANAF Thermochemical Tables, 3rd Edn, Vol. 14 (1985).
17. G. I. BATALIN and N. I. KUZMENKO, *Russ. J. Phys. Chem.* **56** (1982) 1586.
18. J. G. LI, D. CHATAIN, L. COUDURIER and N. EUSTATHOPOULOS, *J. Mater. Sci. Lett.* **7** (1988) 961.
19. B. DREVET, D. CHATAIN and N. EUSTATHOPOULOS, *J. Chim. Phys.* **87** (1990) 117.
20. J. G. LI, L. COUDURIER and N. EUSTATHOPOULOS, *Rev. Int. Hautes Temp. Réfract (F)* **24** (1987–88) 85.
21. D. CHATAIN, I. RIVOLLET and N. EUSTATHOPOULOS, *J. Chim. Phys.* **83** (1986) 561.
22. K. T. JACOB and C. B. ALCOCK, *Acta Metall.* **20** (1972) 221.
23. A. R. MIEDEMA, F. R. de BOER, R. BOOM and J. W. F. DORLEIJN, *Calphad* **1** (1977) 353.
24. J. G. LI, L. COUDURIER and N. EUSTATHOPOULOS, *J. Mater. Sci.* **24** (1989), 1109.
25. L. E. MURR, in "Interfacial Phenomena in Metals and Alloys" (Addison-Wesley, Reading, Massachusetts, 1975).
26. N. EUSTATHOPOULOS and J. C. JOUD, in "Current Topics in Materials Science", Vol. 4, edited by E. Kaldis (North Holland, Amsterdam, 1980) p. 281.
27. W. D. KINGERY, *J. Amer. Ceram. Soc.* **37** (1954) 42.
28. M. McLEAN and E. D. HONDROS, *J. Mater. Sci.* **6** (1971) 19.
29. B. GALLOIS, thesis, Carnegie Mellon University, Pittsburgh, USA (1980).
30. P. NIKOLOPOULOS, *J. Mater. Sci.* **20** (1985) 3993.
31. S. H. OVERBURY, P. A. BERTRAND and G. A. SOMORJAI, *Chem. Rev.* **75** (1975) 547.



*Received 5 April*
*and accepted 10 October 1990*